A general property of solutions of Eulerian hydrodynamic equations: the formation of discontinuities at a liquid surface

N. A. Inogamov[1)]

L. D. Landau Institute of Theoretical Physics, Russian Academy of Sciences, 117940 Moscow, Russia

(Submitted 10 October 1994; resubmitted 30 November 1994)
Pis'ma Zh. Eksp. Teor. Fiz. **61**, No. 1, 28–33 (10 January 1995)

The evolution of a boundary η is studied. A collapse is observed, consisting of the spontaneous formation of singularities on solutions of the Cauchy problem of a general type which are initially smooth everywhere. This collapse occurs after a finite time t_{sing}. An important advance is that the analysis is based on equations which incorporate a realistic strong nonlinearity. (The weakly nonlinear approximation is valid when the singularities are far from a boundary. A strong nonlinearity is taken into account by carrying out a high-order expansion and analyzing the convergence of the results as the order of the expansion varies.) In addition, a singularity has been observed in valleys between surges or "between fingers." (The onset of singularities at points of acoustic catastrophes, corresponding to surges of the liquid, has been predicted previously on the basis of weakly nonlinear approximations which lead to equations analogous to gasdynamic equations with a negative pressure and an imaginary sound velocity. Liquid surges or jets are often called "fingers.") Details of the stages before and after the collapse are reported.

Questions concerning the dynamics of a free boundary or contour dynamics arise in research on instabilities in pinches,[1] in tokamaks,[2] in laser throwing,[3,4] and in many other extremely important physical applications. There is also interest in the fundamental problems involved in studying the structure of solutions of the equations of mathematical physics, in particular, for hydrodynamic collapse in the Eulerian equations. This topic has received a great deal of attention recently, as can be seen from simply the most recent papers.[5,6]

We consider general solutions of the classical[7–9] boundary-value problem

$$\Delta\varphi=0, \quad k(x,t)=0, \quad d(x,t)=0, \quad k=K(x,y,t)|_{y=\eta(x,t)}, \quad d=D(x,y,t)|_{y=\eta(x,t)},$$

$$K=\eta_t+\varphi_x\eta_x-\varphi_y, \quad D=\varphi_t+(\varphi_x^2+\varphi_y^2)/2+p/\rho-gy, \quad p|_\eta=0, \quad \varphi(x,y\to\infty)\to 0, \tag{1}$$

where the curve $\eta\leqslant y<\infty$ bounds the liquid, $k=0$ and $d=0$ are respectively kinematic and dynamic boundary conditions, φ is the velocity potential ($v=\nabla\varphi$), and g is the y component of the acceleration due to gravity.

We expand the solutions of this problem in series as follows:

$$f=\sum_{n=1}^{N}[A_n(t)/n]\exp[n(S_0+iz)],\quad f=\varphi+i\psi,\quad z=x+iy,\quad \eta=\sum_{n=0}^{N}S_n x^{2n}. \quad (2)$$

We see from (1) and (2) that the values $g=1$, 0, and -1 correspond to standing gravity waves, a Richtmyer–Meshkov instability, and a Rayleigh–Taylor instability, respectively. In studies of evolution of this type it is always tacitly assumed that the amplitudes of the higher harmonics fall off exponentially at the initial time: $A_n(0)\sim c^{-n}$, with $c>1$ at $n\gg 1$. One can then show that small-scale instabilities cannot disrupt the smoothness of the solutions over a finite time.

We write the left sides of boundary conditions (1) as series in x^2: $k=\Sigma k_n x^{2n}$, $d=\Sigma d_n x^{2n}$, where $n=0,1,...,N$. According to (1), the evolution of the contour η is then governed by the dynamic system $k_n=0$, $d_n=0$. After expansions (2) are substituted into this system, and also after some lengthy transformations, the system becomes

$$\dot{A}_i=\sum_{j=1}^{N}(G^{-1})_{ij}\left(gS_j+\sum_{k=1}^{N}\sum_{m=1}^{N}M_{jkm}A_kA_m\right),\quad \dot{S}_i=\sum_{j=1}^{N}D_{ij}A_j,\quad i=1,2,...,N. \quad (3)$$

The coefficients G, M, and D in (3), which are polynomials in S_n, are calculated for $N\leq 6$. In higher-order approximations these polynomials become excessively complicated and require a separate representation.

In the single-mode approximation ($N=1$), system (3) reduces to the equation $dU/dR=2(UR+g)/[R(R-1)(R-3)]$, where $U=A_1^2$, and $R=-(2S_1)^{-1}$ is the radius of curvature of the curve $\eta(x,t)$ at the point $x=0$. We then find a description of the case $g=-1$ which is far simpler and more comprehensive than the earlier description.[10,11] It is also possible to completely integrate the trajectories in the case $g=0$; this case has not been considered previously.[2)]

In the higher-multimode approximations, $1<N\leq 6$, system (3) has been integrated by numerical methods. It has been found that the trajectories which have physical meaning and which evolve from a broad neighborhood (on the order of unity) of the point of hydrostatic equilibrium are attracted to the hypersurface G_{crit}, on which the matrix of coefficients G_{ij} becomes degenerate at accelerations $\dot{A}_n$[see (3)]. The expressions for the determinants $|G|_N$, where N is the order of the approximation, are complicated polynomials in S_n:

$$|G|_1=-\frac{1}{2}-S_1,\quad \{2\};\quad |G|_2=-\frac{1}{8}-\frac{19S_1}{24}-3S_1^2 2-\frac{S_1^3}{2}-\frac{S_2}{2},\quad \{5\};$$

$$|G|_3=\frac{1}{48}+\frac{389S_1}{1440}+...,\quad \{14\};\quad |G|_4=\frac{1}{384}+\frac{6893S_1}{120960}+\frac{3927773S_1^2}{7257600}+...,\quad \{41\};$$

$$|G|_5=-\frac{1}{3840}-\frac{83341S_1}{9676800}-\frac{790583881S_1^2}{6096384000}-...,\quad \{126\}$$

$$|G|_6 = -\frac{1}{46080} - \frac{6448957S_1}{6386688000} - \ldots - \frac{127S_1S_4S_6}{576} - \frac{7S_1^2S_4S_6}{16}$$
$$- \frac{13S_1^3S_4S_6}{48} - \frac{S_2S_4S_6}{48}, \quad \{385\}.$$

The numbers in braces (curly brackets) here are the numbers of terms in the corresponding polynomials.

As the hypersurface G_{crit} is approached, the values of $\dot{A}_n$ increase without bound, and the Fourier expansion (2) of the potential diverges. Since this expansion converges in the half-plane $y > y_{\text{up}}$, which is bounded from below by the y coordinate of the uppermost singularity of the potential, y_{up}, the singularity S_{up} comes quite close to the surface η.

Comparison of the calculations with $N=1$ and $N>1$ leads to the conclusion that there is a qualitative difference between these two cases. At $N=1$, there are always solutions of (3): $0 \leqslant t < \infty$. In the limit $t \to \infty$, these solutions tend toward an asymptotic solution. At $N>1$, on the other hand, smooth solutions are everywhere restricted to a finite time interval: $0 \leqslant t < t_{\text{sing}}$. At the time t_{sing}, the trajectories reach G_{crit}.

Much effort was devoted to a thorough study of the convergence of the results at high values of N. We found the differences between the trajectories and the times t_{sing} corresponding to successive values of N, i.e., the differences between the $N=6$ and $N=5$ cases, between the $N=5$ and $N=4$ cases, etc. It turns out that these differences fall off rapidly with increasing N. This decrease means that the results do indeed reflect the actual specific features of the system under study.

The fact that the upper singularity S_{up} approaches the boundary η at the valley vertex S_0 (Fig. 1, a and b), and the fact that the acceleration $\dot{A}_n$ becomes infinite point to the explanation offered below for the collapse. The same facts suggest certain conclusions regarding the structure of the solution after the collapse.

Let us consider the boundary $\eta(x,t)$ and its curvature; see Fig. 1, a and a′, where $R(x,t) = (\sqrt{1+\eta_x^2})^3/\eta_{xx}$. The sign of R and the spatial position of the region occupied by the liquid are such that valleys which are concave toward the liquid correspond to regions with $R<0$, while valleys which are convex toward the liquid correspond to jets j with $R>0$ (Fig. 1, a and a′). The most concave region on η is the neighborhood of the vertex S_0; see the maxima on the plot of $R(x,t)$ versus x at the points $2\pi n$. The isobars thus become more closely spaced near S_0, and there is a self-sharpening of the vertex. At the time of collapse, t_{sing}, the radius R vanishes at the points $x = 2\pi n$ (Fig. 1b′), and the η curve forms an arrowhead with a vertex angle δ (Fig. 1b and Fig. 2). Here τ is the tangent to η at S_0. Near the time t_{sing} and also near the vertex, the precollapse solution is self-similar.[3)]

The formation of the wedge-shaped vertex marks the end of the precollapse solution. At this point, the vertex breaks up. A bubble b_N and two cusps, S^l_{cusp} and S^τ_{cusp}, form (Fig. 2). The boundary of bubble b_N is a section of the newly formed boundary η. The reason is that the Lagrange particles which are at the boundary b_N were collected at S_0 at the time of collapse.

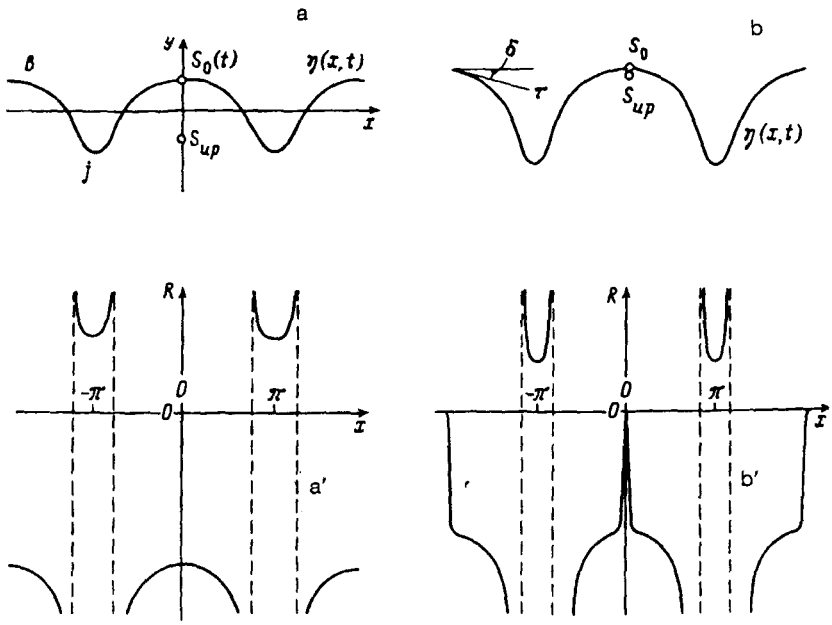

FIG. 1. Precollapse evolution of the shape of the boundary and its curvature. a, b: Types of η. $S_0(t)$ is the y coordinate of the valley vertex in the laboratory coordinate system [see expansion (2)]. The point S_{up} corresponds to the uppermost of the set of singularities of the potential. b—Valleys; j—jets or surges. a′,b′: Plot of $R(x,t)$ versus x. Alternation of concave and convex regions. Values $R=\infty$ correspond to inflection points of η. b, b′: Proximity of the singularity S_{up} to the vertex S_0 and formation of a bend with an angle δ at S_0 at the time of collapse, t_{sing}.

The cusp vertices $S^{l,\tau}_{cusp}$ move by inertia, since we have $\nabla p=0$ in their vicinity. It follows from self-similarity considerations that the increment in the velocity of vertex S_0 at the time t_{sing} cannot be a finite quantity. Accordingly, the vertices of the left and

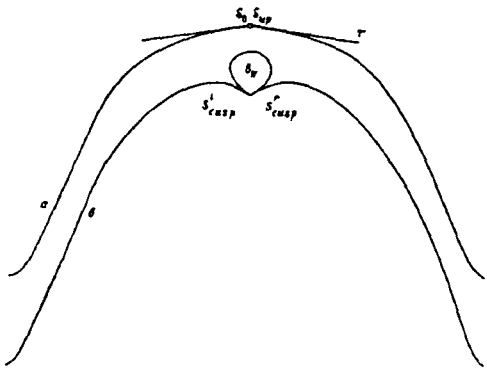

FIG. 2. Postcollapse evolution of $\eta(x,t)$. Curve a: $t=t_{sing}$; tangents have been drawn from the vertex S_0. At the time of collapse, the points S_{up} and S_0 merge. Curve b: $t>t_{sing}$. The cusps S^l_{cusp} and S^r_{cusp} coincide.

right cusps coincide ($S^l_{\text{cusp}} = S^\tau_{\text{cusp}}$; Fig. 2), and their trajectory is described by the inertial expression: $y_{\text{cusp}}(t) = S_0(t_{t_{\text{sing}}}) + (t - t_{t_{\text{sing}}})\dot{S}_0(t_{t_{\text{sing}}}) + (t - t_{t_{\text{sing}}})^2 g/2$.

Single cusps are usually branch points of the potential, at which cuts which are lines of distributed sources terminate. In the case at hand, the cusp points are double points. It is possible that, again in this case, the singularity S_{up} near S_0 is a branch point and that a cut approaches the cusps $S^{l,\tau}_{\text{cusp}}$ at $t > t_{\text{sing}}$.

A detailed comparison (Fig. 3) has been made of theoretical data found through an integration of (3) with the data from numerical simulations carried out by A. V. Chekhlov at the request of the authors. These simulations were carried out with the help of the long-established codes based on an artificial compressibility[12] and finite-size particles.[13] The calculations carried out by these two types of codes, which are completely different, turned out to be in satisfactory agreement. It was also found that the theory is supported by the simulations. Specifically, the shapes of the boundary and its velocities at $t < t_{\text{sing}}$ are in agreement, as are the values of the time t_{sing}. The simulations also reveal bubbles b_N and cusps S^l_{cusp} and S^τ_{cusp} at $t > t_{\text{sing}}$.

We would like to point out an effect associated with the lower liquid. Since it is incompressible, it must enter the expanding bubble b_N. Thus the neighborhood of the points S_{cusp} (Fig. 2) either ruptures or stretches out and presses against the surface of b_N. If the density of the lower liquid is $\rho_l = 0$, this neighborhood is infinitesimal.

This theory covers the case in which the density ratio ($\mu = \rho_l/\rho$) of the liquids on the two sides of boundary η is zero. When the numerical codes of Refs. 12 and 13 are used, on the other hand, it is necessary to restrict the calculations to cases with nonzero μ. The reason is that the efficiency and the reliability of the calculations suffer at exceedingly small values of μ. It is accordingly necessary to discuss the effect of small but nonzero values of μ on the results.

Let us compare the solutions with $\mu = 0$ and $\mu \ll 1$. At $\mu \neq 0$, a mushroom-shaped region forms at the end of jet j (Fig. 1a) as time elapses.[14] An estimate of the total perturbation amplitude y_Σ (i.e., the vertical distance between the valley vertex S_0 and the jet vertex j; Fig. 1a) at the time at which the mushroom forms, t_{mush}, is given by the expression[14] $y_\Sigma(t_{\text{mush}}) \approx y_{\text{mush}} \approx 0.27\mu^{-2/3}$. Analysis of the numerical simulations indicates that the process by which the mushroom forms consists of the formation of a bend on η, a discontinuity in η at the bend vertex, and the appearance of a bubble (the arc between points a and b in Fig. 3) and the two cusps a and b. Figure 3 shows the case with $\mu = 0.1$. Here we have $t_{\text{mush}} \approx 1.5$. The estimate of $y_\Sigma(t_{\text{mush}})$ given above is 50% too high.

At $y_\Sigma < y_{\text{mush}}$, the solutions with $\mu = 0$ and $\mu \ll 1$ differ only slightly. Consequently, the theory with $\mu = 0$ also describes cases with $\mu \ll 1$. At $y_\Sigma > y_{\text{mush}}$, the solution breaks up into two subregions: valleys and jets. In the valley subregion of interest here (in connection with the question of a singularity at a valley), the solutions with $\mu = 0$ and $\mu \ll 1$ again differ only slightly,[4)] and the theory derived here is applicable. The theoretical results converge well as N increases. Comparison of the theory and the numerical simulation shows that the corresponding shapes of η agree very accurately away from the mushroom subregion, i.e., above point b in Fig. 3.

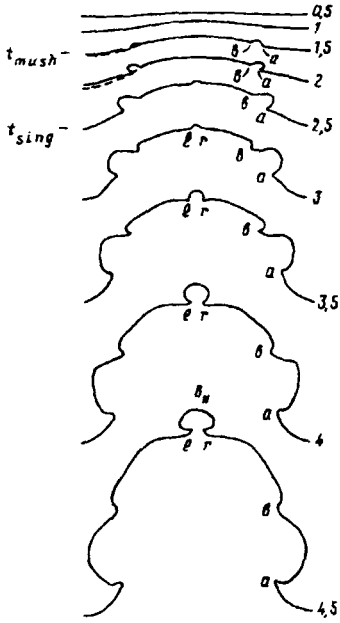

FIG. 3. Comparison of the theoretical evolution of η (dashed curves; only symmetric halves are shown) with the experimental evolution (solid curves). Arrival of the singularities at the boundary and the formation of discontinuities and cusps. The curve labels are the times. The letters l and τ represent the points S^l_{cusp} and S^τ_{cusp}, respectively. Since a value $\mu \neq 0$ was used in the numerical simulation, these are distinct points, rather than double points, as in Fig. 2. A bubble b_N can be seen clearly at the valley vertex; it is bounded by the points l and τ. It arises at $t > t_{sing}$. For this particular version we have $t_{sing} \approx 2.5$. The theory predicts $t_{sing} \approx 2.7$. The reason for the formation of cusps a and b is the value $\mu \neq 0$ (see the text proper).

The reason why the cusps are separated from each other (compare Figs. 2 and 3) is the value $\mu \neq 0$. As the light liquid flows into the growing bubbles, the dynamic pressure $\rho_l v^2$ exerted by the rapidly moving light liquid has an effect. It causes a curling of the ends of the cusps.

I wish to thank S. I. Anisimov for a useful discussion and A. V. Chekhlov and A. Yu. Dem'yanov for assistance in the numerical calculations. This study had financial support from the Russian Fund for Fundamental Research (Project Code 93-02-3630).

[1]E-mail: Nail@landau.ac.ru

[2)]In other words, an analog of the Layzer solution[10] for the case of the Richtmyer–Meshkov instability is found and integrated.

[3)]Determining the angle of the bend and the self-similarity characteristics will require a numerical simulation on meshes finer than those discussed below.

[4)]The solution found for a zero density of the second liquid is of course not valid for describing the mushroom. The mushroom is described by a solution which follows from the theory of periodic jets (see the last section in Ref. 14).

[1] A. B. Bud'ko *et al.*, Zh. Eksp. Teor. Fiz. **96**, 140 (1989) [Sov. Phys. JETP **69**, 76 (1989)].
[2] S. V. Bazdenko and O. P. Pogutse, JETP Lett. **57**, 423 (1993).
[3] S. W. Haan, Phys. Fluids B **3**, 2349 (1991).
[4] V. B. Rozanov *et al.*, Preprint 56, P. N. Lebedev Physics Institute, Russian Academy of Sciences, Moscow, 1990.
[5] E. A. Kuznetsov *et al.*, Phys. Lett. A **182**, 387 (1993).
[6] E. A. Kuznetsov *et al.*, Phys. Rev. E **49**, 1283 (1994).
[7] L. D. Landau and E. M. Lifshitz, *Fluid Mechanics* (Pergamon, Oxford, 1987).
[8] D. H. Sharp, Physica D **12**, 3 (1984).

[9]H. J. Kull, Phys. Rep. **206**, 197 (1991).
[10]D. Layzer, Astrophys. J **122**, 1 (1955).
[11]H. J. Kull, Phys. Rev. Lett. **51**, 1434 (1983).
[12]N. A. Inogamov and A. V. Chekhlov, *Proc. of the 4th Internat. Workshop on the Phys. of Compressible Turbulent Mixing*, ed. by P. F. Linden, D. L. Youngs, and S. B. Dalziel (Cambridge Univ. Press, Cambridge, England, 1993), p. 50.
[13]O. M. Belotserkovskiĭ and Yu. M. Davydov, *The Method of Finite-Size Particles in Gas Dynamics* [in Russian] (Nauka, Moscow, 1982).
[14]S. I. Anisimov *et al.*, Russ. J. Comp. Mech. **1**, No. 2 (1993).

Translated by D. Parsons